



## Original article

## 1,5-Diphenylpenta-2,4-dien-1-ones as potent and selective monoamine oxidase-B inhibitors

Nicoletta Desideri<sup>a,\*</sup>, Rossella Fioravanti<sup>a</sup>, Luca Proietti Monaco<sup>a</sup>, Mariangela Biava<sup>a</sup>, Matilde Yáñez<sup>b</sup>, Francesco Ortuso<sup>c</sup>, Stefano Alcaro<sup>c</sup><sup>a</sup> Dipartimento di Chimica e Tecnologie del Farmaco, Sapienza – Università di Roma, P.le Aldo Moro 5, 00185 Rome, Italy<sup>b</sup> Departamento de Farmacología and Instituto de Farmacia Industrial, Facultad de Farmacia, Universidad de Santiago de Compostela, Campus Universitario Sur, E-15782 Santiago de Compostela, La Coruña, Spain<sup>c</sup> Dipartimento di Scienze della Salute, Università "Magna Græcia" di Catanzaro, Campus Universitario "S. Venuta", Viale Europa, 88100 Catanzaro, Italy

## ARTICLE INFO

## Article history:

Received 3 July 2012

Received in revised form

6 November 2012

Accepted 7 November 2012

Available online 15 November 2012

## Keywords:

1,5-Diphenylpenta-2,4-dien-1-ones

Monoamine oxidase

hMAO-B inhibitors

Structure–activity relationship

Docking

## ABSTRACT

A series of (2*E*,4*E*)-1-(2-hydroxyphenyl)-5-phenylpenta-2,4-dien-1-ones (**3a–r**) and (2*Z*,4*E*)-3-hydroxy-1-(2-hydroxyphenyl)-5-phenylpenta-2,4-dien-1-ones (**6a–l**) were synthesized and evaluated *in vitro* as inhibitors of the two human Monoamine oxidase (hMAO) isoforms, MAO-A and MAO-B. Most of the compounds showed a selective MAO-B inhibitory activity in the nanomolar or low micromolar range. (2*E*,4*E*)-5-(4-Chlorophenyl)-1-(2-hydroxy-4-methoxyphenyl)penta-2,4-dien-1-one (**3g**) and (2*E*,4*E*)-5-(4-chlorophenyl)-1-(2,4-dihydroxyphenyl)penta-2,4-dien-1-one (**3h**) were the most potent hMAO-B inhibitors exhibiting IC<sub>50</sub> of 4.51 nM and 11.35 nM, respectively, coupled with high selectivity. Moreover, partial recovery of MAO-B activity was observed after repeated washing in the presence of isatin (reversible inhibitor) and compounds **3g** and **3h** suggesting a reversible inhibition of the enzyme. Molecular mechanics and quantum chemistry methods were used to elucidate the MAO recognition of the most active inhibitors **3g** and **3h**.

© 2012 Elsevier Masson SAS. All rights reserved.

## 1. Introduction

Monoamine oxidase (MAO, EC 1.4.3.4) is a flavoenzyme that catalyzes the deamination of a broad spectrum of biogenic and xenobiotic amines. Two isoforms of MAOs have been identified and designated as MAO-A and MAO-B. The MAO isozymes are products of separate genes and they share approximately 70% amino acid sequence identity [1]. Studies on X-ray crystallographic structures of human MAO-A and MAO-B indicate that 6 of the 16 amino acid residues comprising the active sites differ between the two enzymes [2,3]. For these reasons, MAO-A and MAO-B have different substrate and inhibitor specificities. MAO-A preferentially metabolizes the neurotransmitters, serotonin, epinephrine and norepinephrine, and it is selectively inhibited by clorgyline. MAO-B are predominantly involved in the metabolism of benzylamine and β-phenylethylamine, and it is selectively inhibited by selegiline and rasagiline. Dopamine and tyramine are considered to be a substrate for both isozymes [4]. Although in humans both isozymes are expressed in most peripheral tissues and organs, MAO-A is

preponderant in placenta, lung and small intestine, while MAO B is the only isoform in platelets and lymphocytes. In brain MAO B (present in glial cells) predominates over MAO A [1]. These properties determine the therapeutic potential of MAO inhibitors. MAO-A inhibitors have therapeutic utility for the treatment of depression [5] whereas MAO-B inhibitors are used with L-DOPA and/or dopamine agonists in the symptomatic treatment of Parkinson's disease [6,7], and are potential drugs in the therapy of Alzheimer's disease (AD) [8,9]. However, the first generation of non selective and irreversible MAO inhibitors was characterized by adverse side-effects such as serious hypertensive crisis following the ingestion of dietary tyramine. The efforts devoted to the discovery of safer inhibitors led to the new generation of MAO inhibitors characterized by the selectivity against MAO isoforms and in some cases by the reversibility of action. As the ideal drug candidate has not been achieved, researchers continued to explore this field.

Recently, we reported new series of MAO inhibitors related to natural compounds as flavones, thioflavones and flavanones [10], homoisoflavones [11], and chalcones [12], the biogenetic precursors of flavonoids. The potent and selective hMAO-B inhibitory activity of several synthetic chalcones [12] and of 1,4-diphenyl-2-butene [13], prompted us to design and test against hMAO-A and hMAO-B isoforms a series of structurally related (2*E*,4*E*)-1-(2-

\* Corresponding author. Tel.: +39 06 49913892; fax: +39 06 49693268.

E-mail address: [nicoletta.desideri@uniroma1.it](mailto:nicoletta.desideri@uniroma1.it) (N. Desideri).

hydroxyphenyl)-5-phenylpenta-2,4-dien-1-ones (**3a–r**) and (2*Z*,4*E*)-3-hydroxy-1-(2-hydroxyphenyl)-5-phenylpenta-2,4-dien-1-one (**6a–j**).

## 2. Results and discussion

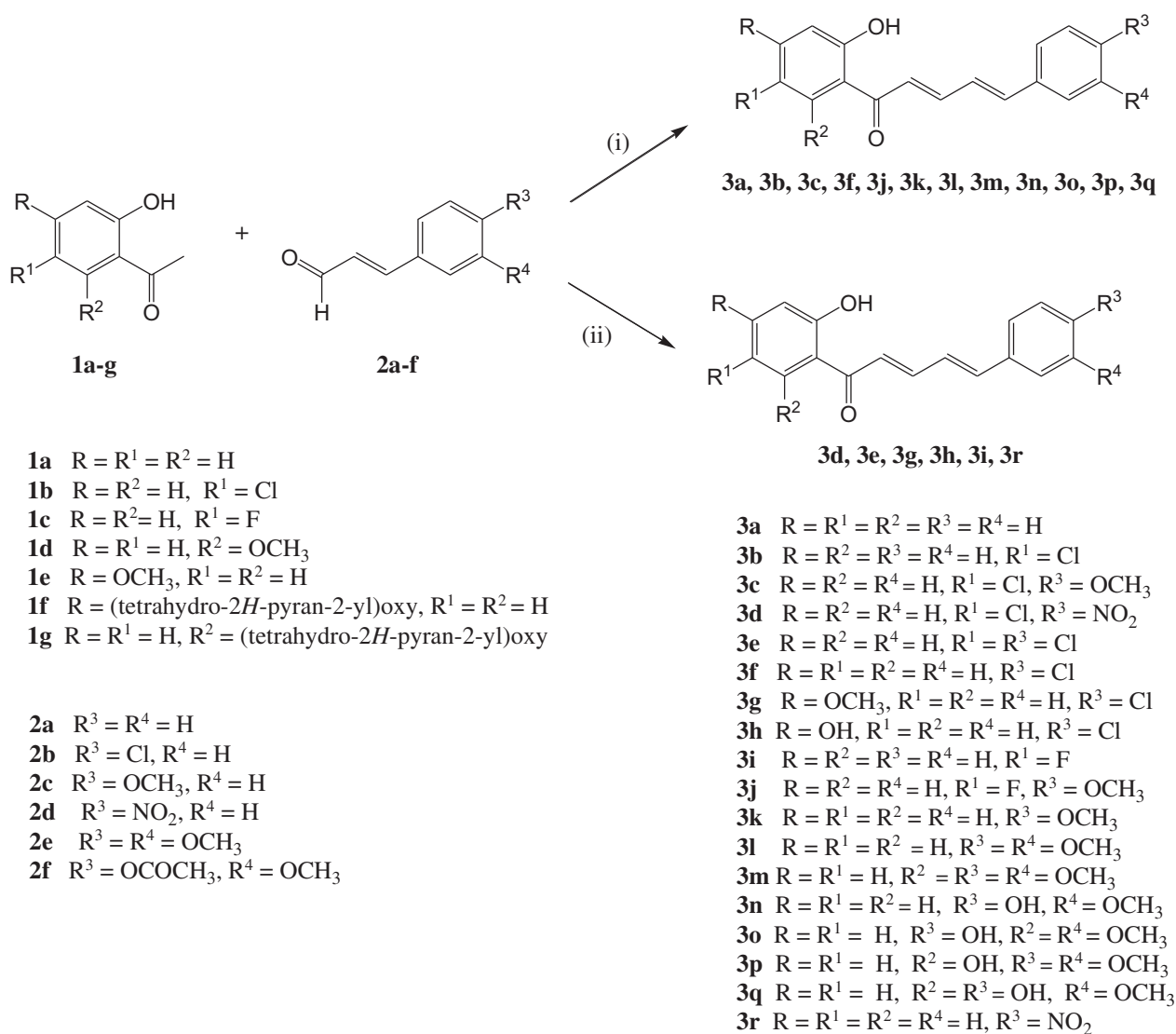
### 2.1. Chemistry

(2*E*,4*E*)-1-(2-Hydroxyphenyl)-5-phenylpenta-2,4-dien-1-ones (**3a–r**) were synthesized by base-catalyzed reaction of the appropriate 2-hydroxyacetophenone (**1a–g**) and substituted cinnamaldehyde (**2a–f**). The condensation was performed in hydroalcoholic sodium hydroxide or in methanol using barium hydroxide octahydrate as base (Scheme 1). The deprotection of

hydroxyl groups to obtain the compounds **3h**, **3n**, **3o**, **3p** and **3q** was achieved during the work up of the reaction mixture.

(2*Z*,4*E*)-3-Hydroxy-1-(2-hydroxyphenyl)-5-phenylpenta-2,4-dien-1-ones (**6a–j**) were prepared according to the two step procedure shown in Scheme 2. The appropriate 2-hydroxyacetophenone (**1a–e**) was first converted into the corresponding 2-acetylphenyl (*E*)-cinnamate (**5a–j**) by treatment with substituted cinnamic acid (**4a–g**) in the presence of phosphoryl chloride, in dry pyridine. In the second step, the Baker–Venkataraman rearrangement of the formed ester (**5a–j**) into desired **6a–j** was achieved in the presence of potassium carbonate, in dry acetone.

The hydroxy-analogs **6k** and **6l** were achieved by treatment with boron tribromide of a solution of the corresponding methoxy derivatives **6e** and **6f** in dry dichloromethane (Scheme 3).



<sup>a</sup>Reagents and conditions: (i) 60% NaOH, MeOH, r.t. 48 h; for **3n** and **3o** 60 °C 5 h; (ii) Ba(OH)<sub>2</sub> · 8H<sub>2</sub>O, MeOH, 50 °C, 5 h.

Scheme 1.



evaluated by measuring the fluorescence generated by resorufin using the general procedure described previously by us [14].

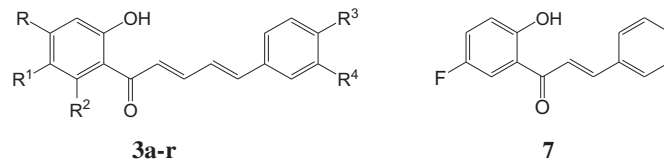
The hMAO-A and hMAO-B inhibition data and the selectivity indexes (SI =  $IC_{50}$  hMAO-A/ $IC_{50}$  hMAO-B) of the (2*E*,4*E*)-1-(2-hydroxyphenyl)-5-phenylpenta-2,4-dien-1-ones (**3a–r**) and (2*Z*,4*E*)-3-hydroxy-1-(2-hydroxyphenyl)-5-phenylpenta-2,4-dien-1-ones (**6a–l**) are reported in Tables 1 and 2, respectively, together with the results obtained for the reference inhibitors (clorgyline, selegiline, isatin, iproniazid and moclobemide).

Generally, the new tested compounds selectively inhibited the enzymatic activity of hMAO-B in the nanomolar or low micromolar range. The most interesting compound of the entire series of inhibitors was (2*E*,4*E*)-5-(4-chlorophenyl)-1-(2-hydroxy-4-methoxyphenyl)penta-2,4-dien-1-one **3g**, showing potent hMAO-B activity and high selectivity ( $IC_{50}$  = 4.51 nM, SI > 22,173). Within the series of (2*E*,4*E*)-1-(2-hydroxyphenyl)-5-phenylpenta-2,4-dien-1-ones (**3a–r**), in addition to the affinity for hMAO-B, some derivatives (**3f**, **3h**, **3n**, **3o**, **3p** and **3q**) are also able to inhibit hMAO-A in the micromolar range. These compounds demonstrate a different extent of hMAO-B selectivity, showing SIs ranging from 1.5 to 1354. With the exception of **3f**, these analogs bear at least another hydroxyl group in the aromatic rings in addition to the hydroxyl group in position 2. The same behavior was observed for related chalcones and homoisoflavones previously studied by us [11,12]. It is noteworthy that the replacement of

the methoxyl group in the potent hMAO-B inhibitor **3g** with the hydroxyl group in the same position resulted in compound **3h**, able to inhibit both hMAO isoforms. Although about 2-fold less potent than **3g** as hMAO-B inhibitor, **3h** remain potent in the nanomolar range and endowed with an excellent selectivity ( $IC_{50}$  = 11.35 nM, SI = 1354). In this series of penta-2,4-dien-1-ones (**3a–r**), only the trimethoxy analog **3m** was essentially inactive against both isoforms up to the highest concentration tested (100  $\mu$ M). The replacement of one or two methoxyl groups in **3m** with hydroxyl groups results in compounds (**3o**, **3p** and **3q**) with affinity toward both hMAO isoforms. On the contrary, the removal of one or two methoxyl groups (compounds **3i** and **3k**, respectively) restored only the MAO-B affinity in the micromolar range. The replacement of the 3-methoxyl group in **3i** with the hydroxyl group to obtain compound **3n**, confirmed the ability of poly-hydroxy substituted analogs to inhibit both isoforms.

The introduction of a hydroxyl group in position 3 of the chain results in the (2*Z*,4*E*)-3-hydroxy-1-(2-hydroxyphenyl)-5-phenylpenta-2,4-dien-1-ones (**6a–l**). This structural modification produced a loss of the inhibitory activity or a marked reduction in potency with respect to unsubstituted (2*E*,4*E*)-1-(2-hydroxyphenyl)-5-phenylpenta-2,4-dien-1-ones (**3a–r**) (Table 2). The only exception was represented by (2*Z*,4*E*)-1-(5-fluoro-2-hydroxyphenyl)-3-hydroxy-5-phenylpenta-2,4-dien-1-one (**6d**) that showed a potent hMAO-B inhibitory activity slightly higher

**Table 1**  
hMAO inhibitory activities and selectivity indexes of (2*E*,4*E*)-1-(2-hydroxyphenyl)-5-phenylpenta-2,4-dien-1-ones (**3a–r**), (E)-1-(5-fluoro-2-hydroxyphenyl)-3-phenylprop-2-en-1-one (**7**) and reference inhibitors.



Compd	R	R <sup>1</sup>	R <sup>2</sup>	R <sup>3</sup>	R <sup>4</sup>	MAO-A ( $IC_{50}$ ) <sup>a</sup>	MAO-B ( $IC_{50}$ ) <sup>a</sup>	SI <sup>d</sup>
<b>3a</b>	H	H	H	H	H	<sup>e</sup>	105.51 ± 5.68 nM	>948 <sup>h</sup>
<b>3b</b>	H	Cl	H	H	H	<sup>e</sup>	54.77 ± 2.63 nM	>1826 <sup>h</sup>
<b>3c</b>	H	Cl	H	OCH <sub>3</sub>	H	<sup>e</sup>	153.14 ± 6.21 nM	>653 <sup>h</sup>
<b>3d</b>	H	Cl	H	NO <sub>2</sub>	H	<sup>e</sup>	1.08 ± 0.08 $\mu$ M	>93 <sup>h</sup>
<b>3e</b>	H	Cl	H	Cl	H	<sup>e</sup>	1.46 ± 0.13 $\mu$ M	>68 <sup>h</sup>
<b>3f</b>	H	H	H	Cl	H	37.73 ± 1.57 $\mu$ M <sup>b</sup>	860.46 ± 43.18 nM	44
<b>3g</b>	OCH <sub>3</sub>	H	H	Cl	H	<sup>e</sup>	4.51 ± 0.28 nM	>22,173 <sup>h</sup>
<b>3h</b>	OH	H	H	Cl	H	15.37 ± 1.18 $\mu$ M <sup>b</sup>	11.35 ± 0.73 nM	1354
<b>3i</b>	H	F	H	H	H	<sup>e</sup>	75.84 ± 7.66 nM	>1319 <sup>h</sup>
<b>3j</b>	H	F	H	OCH <sub>3</sub>	H	<sup>e</sup>	725.92 ± 31.56 nM	>138 <sup>h</sup>
<b>3k</b>	H	H	H	OCH <sub>3</sub>	H	<sup>f</sup>	1.81 ± 0.15 $\mu$ M	>55 <sup>h</sup>
<b>3l</b>	H	H	H	OCH <sub>3</sub>	OCH <sub>3</sub>	<sup>f</sup>	14.61 ± 2.18 $\mu$ M	>6.8 <sup>h</sup>
<b>3m</b>	H	H	OCH <sub>3</sub>	OCH <sub>3</sub>	OCH <sub>3</sub>	<sup>e</sup>		
<b>3n</b>	H	H	H	OH	OCH <sub>3</sub>	1.56 ± 0.19 $\mu$ M <sup>b</sup>	501.66 ± 49.19 nM	3.1
<b>3o</b>	H	H	OCH <sub>3</sub>	OH	OCH <sub>3</sub>	1.03 ± 0.25 $\mu$ M <sup>b</sup>	486.35 ± 43.36 nM	2.1
<b>3p</b>	H	H	OH	OCH <sub>3</sub>	OCH <sub>3</sub>	25.16 ± 1.96 $\mu$ M <sup>b</sup>	1.45 ± 0.16 $\mu$ M	17
<b>3q</b>	H	H	OH	OH	OCH <sub>3</sub>	1.43 ± 0.22 $\mu$ M <sup>c</sup>	969.44 ± 87.45 nM	1.5
<b>3r</b>	H	H	H	NO <sub>2</sub>	H	<sup>e</sup>	160.32 ± 12.48 nM	>624 <sup>h</sup>
<b>7</b>	H	F	H	H	H	<sup>f</sup>	667.89 ± 59.32 nM	>150 <sup>h</sup>
Clorgyline						4.46 ± 0.32 nM <sup>b</sup>	61.35 ± 1.13 $\mu$ M	0.000073
Selegiline						67.25 ± 1.02 $\mu$ M <sup>b</sup>	19.60 ± 0.86 nM	3431
Isatin						<sup>f</sup>	21.07 ± 1.47 $\mu$ M	>4.7 <sup>h</sup>
Iproniazid						6.56 ± 0.76 $\mu$ M	7.54 ± 0.36 $\mu$ M	0.87
Moclobemide						361.38 ± 19.3 $\mu$ M	<sup>g</sup>	<0.36 <sup>i</sup>

<sup>a</sup> All  $IC_{50}$  values shown in this table are the mean ± S.E.M. from five experiments. Level of statistical significance.

<sup>b</sup>  $P < 0.01$  or.

<sup>c</sup>  $P < 0.05$  versus the corresponding  $IC_{50}$  values obtained against MAO-B, as determined by ANOVA/Dunnett's.

<sup>d</sup> SI: hMAO-B selectivity index =  $IC_{50}$ (hMAO-A)/ $IC_{50}$ (hMAO-B).

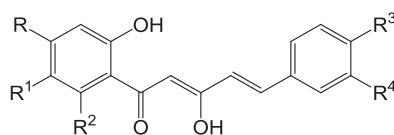
<sup>e</sup> Inactive at 100  $\mu$ M (highest concentration tested).

<sup>f</sup> 100  $\mu$ M inhibits the corresponding MAO activity by approximately 40–50%. At higher concentration the compounds precipitate.

<sup>g</sup> Inactive at 1 mM (highest concentration tested).

<sup>h</sup> Values obtained under the assumption that the corresponding  $IC_{50}$  against MAO-A is the highest concentration tested (100  $\mu$ M).

<sup>i</sup> Values obtained under the assumption that the corresponding  $IC_{50}$  against MAO-B is the highest concentration tested (1 mM).

**Table 2**hMAO inhibitory activities and selectivity indexes of (2*Z*,4*E*)-3-hydroxy-1-(2-hydroxyphenyl)-5-phenylpenta-2,4-dien-1-ones (**6a–l**) and reference inhibitors.**6a-l**

Compd	R	R <sup>1</sup>	R <sup>2</sup>	R <sup>3</sup>	R <sup>4</sup>	MAO-A (IC <sub>50</sub> ) <sup>a</sup>	MAO-B (IC <sub>50</sub> ) <sup>a</sup>	SI <sup>d</sup>
<b>6a</b>	H	H	H	H	H	e	1.16 ± 0.03 μM	>86 <sup>h</sup>
<b>6b</b>	H	Cl	H	Cl	H	e	e	
<b>6c</b>	H	H	H	Cl	H	e	f	
<b>6d</b>	H	F	H	H	H	e	50.44 ± 4.61 nM	>1983 <sup>h</sup>
<b>6e</b>	H	H	H	OCH <sub>3</sub>	H	e	f	
<b>6f</b>	H	H	H	OCH <sub>3</sub>	OCH <sub>3</sub>	e	e	
<b>6g</b>	H	H	OCH <sub>3</sub>	OCH <sub>3</sub>	OCH <sub>3</sub>	f	e	
<b>6h</b>	H	H	OCH <sub>3</sub>	OH	OCH <sub>3</sub>	3.76 ± 0.42 μM <sup>b</sup>	1.68 ± 0.21 μM	2.2
<b>6i</b>	H	H	H	NO <sub>2</sub>	H	e	2.67 ± 0.28 μM	>37 <sup>h</sup>
<b>6j</b>	H	H	H	CH <sub>3</sub>	H	e	3.77 ± 0.19 μM	>27 <sup>h</sup>
<b>6k</b>	H	H	H	OH	H	1.52 ± 0.04 μM <sup>b</sup>	26.46 ± 1.97 nM	57
<b>6l</b>	H	H	H	OH	OH	431.07 ± 52.45 nM <sup>c</sup>	654.32 ± 61.05 nM <sup>b</sup>	0.66
Clorgyline						4.46 ± 0.32 nM <sup>b</sup>	61.35 ± 1.13 μM	0.000073
Selegiline						67.25 ± 1.02 μM <sup>b</sup>	19.60 ± 0.86 nM	3431
Isatin						f	21.07 ± 1.47 μM	>4.7 <sup>h</sup>
lproniazid						6.56 ± 0.76 μM	7.54 ± 0.36 μM	0.87
Moclobemide						361.38 ± 19.3 μM	g	<0.36 <sup>i</sup>

<sup>a</sup> All IC<sub>50</sub> values shown in this table are the mean ± S.E.M. from five experiments. Level of statistical significance.<sup>b</sup> P < 0.01 or.<sup>c</sup> P < 0.05 versus the corresponding IC<sub>50</sub> values obtained against MAO-B, as determined by ANOVA/Dunnett's.<sup>d</sup> SI: hMAO-B selectivity index = IC<sub>50</sub>(hMAO-A)/IC<sub>50</sub>(hMAO-B).<sup>e</sup> Inactive at 100 μM (highest concentration tested).<sup>f</sup> 100 μM inhibits the corresponding MAO activity by approximately 40–50%. At higher concentration the compounds precipitate.<sup>g</sup> Inactive at 1 mM (highest concentration tested).<sup>h</sup> Values obtained under the assumption that the corresponding IC<sub>50</sub> against MAO-A is the highest concentration tested (100 μM).<sup>i</sup> Values obtained under the assumption that the corresponding IC<sub>50</sub> against MAO-B is the highest concentration tested (1 mM).

than the corresponding (2*E*,4*E*)-1-(5-fluoro-2-hydroxyphenyl)-5-phenylpenta-2,4-dien-1-one (**3i**) (IC<sub>50</sub> = 50.44 nM and 75.84 nM, respectively) and better selectivity (SI > 1983 and >1319, respectively). Also in this series of inhibitors, the compounds substituted with more than one hydroxyl group in the aromatic rings (**6h**, **6k** and **6l**) are able to inhibit both hMAO isoforms. In particular, **6l** was the only hMAO-A inhibitor of both series active in the sub-micromolar range. Moreover, its potency toward B isoform was slightly higher than the potency toward A isoform, resulting in an essentially nonselective compound.

To evaluate whether the most potent hMAO-B inhibitors (**3b**, **3g**, **3h**, **6d**, **6k**) are reversible or irreversible hMAO-B inhibitors, the so-called repeated washing method was used [12]. The results obtained using selegiline (irreversible inhibitor) and isatin (reversible inhibitor) as reference compounds are reported in Table 3.

**Table 3**Reversibility and irreversibility of hMAO-B inhibition of derivatives **3b**, **3g**, **3h**, **6d** and **6k**.

Comp	% MAO-B inhibition	
	Before washing	After repeated washing <sup>a</sup>
<b>3b</b> (100 nM)	58.10 ± 0.10	60.30 ± 2.53
<b>3g</b> (10 nM)	61.34 ± 2.38	37.51 ± 1.13
<b>3h</b> (10 nM)	51.52 ± 3.18	42.02 ± 0.70
<b>6d</b> (100 nM)	62.35 ± 0.45	68.80 ± 3.33
<b>6k</b> (100 nM)	66.70 ± 1.52	68.55 ± 4.39
Isatin (30 μM)	64.31 ± 2.08	31.22 ± 0.91
Selegiline (20 nM)	53.08 ± 1.64	54.63 ± 1.72

Each value is the mean ± S.E.M. from five experiments (n = 5).

<sup>a</sup> Level of statistical significance: P < 0.01 versus the corresponding MAO-B inhibition before washing, as determined by ANOVA/Dunnett's.

The reversibility tests revealed the lack of enzyme activity restoration after repeated washing for compounds **3b**, **6d** and **6k**. Similar results were obtained for selegiline a well-known irreversible MAO-B inhibitor. On the contrary, significant recovery of MAO-B activity was observed after repeated washing of isatin (reversible inhibitor) and compound **3g**. The enzymatic inhibition lowered in a minor extent after repeated washing in the presence of **3h** (Table 3). These results suggest that the novel potent hMAO-B inhibitors **3g** and **3h** are reversible inhibitors.

## 2.3. Molecular modeling studies

With the aim to rationalize the different hMAO inhibition of the analogs **3g** and **3h**, molecular modeling studies were carried out. Following our previous experience [15] we have adopted both molecular mechanics and quantum chemistry methods to elucidate the mechanism of inhibition of previously reported compounds. In particular, the recognition of hMAO-A and -B and the role of the *p*-methoxy substituent, available in the **3g** in replacement of the **3h** hydroxy group, were investigated.

In order to obtain reasonable configuration of both inhibitors into the hMAO-A and -B binding clefts, docking experiment were performed. The top ranked theoretical complex revealed remarkable similarities, actually, in all cases the ligands showed the phenolic ring and the *p*-chlorophenyl moieties respectively positioned toward the FAD cofactor and the entrance gorge surrounded by hydrophobic residues. With the aim to improve the analysis of **3g** and **3h** hMAO recognition, new complexes between our inhibitors and both target isoform models were manually built by means of a 180° rotation of the corresponding top ranked poses. Resulting

structures, after energy optimization and re-scoring procedure, revealed interaction energy remarkably weaker than the original top ranked poses (see Table 1 in Supplementary content). Such a scenario and the docking score (see Figure S1 in Supplementary content) were not in agreement to the experimental  $IC_{50}$  data, as a consequence, each top ranked docking complex was submitted to 12 ns of molecular dynamics (MD). The resulting four trajectories were analyzed in terms of inhibitor target interaction energy and geometry (Section Experimental section) reporting a good qualitative agreement to the experimental inhibition data. Actually, hMAO-B·**3g** resulted as the most energy favored complex with an advantage of about 10 kcal/mol with respect to the hMAO-A·**3g**, conversely predicted as the worst one. The hMAO-B binding energies of **3h** indicated a disadvantage of 3.4 kcal/mol with respect to **3g** on the contrary, into the hMAO-A, 1.2 kcal/mol demonstrated its better recognition than **3g** (see Figure S2 in Supplementary content). The hMAO-B selectivity of the selected compounds was also remarked by computing, during the molecular dynamics runs, the target backbone root mean square deviation (RMSd) with respect to the corresponding starting structures (see Figure S3 in Supplementary content). As reported by the average RMSd values, the target isoform B accommodate both inhibitors with lower perturbation (**3g** = 1.86 Å; **3h** = 2.44 Å) than hMAO-A (**3g** = 3.79 Å; **3h** = 4.12 Å). Such data were not a surprise because it is known [16] that hMAO-B active site ( $\sim 700 \text{ \AA}^3$ ) is larger than hMAO-A one ( $\sim 400 \text{ \AA}^3$ ), and contributed to rationalize the isoform selectivity of our compounds. With the aim to identify the most relevant

residues interacting to **3g** and **3h**, all MD trajectory frames were investigated. The contribution of each residue to the inhibitor binding was expressed as percentage of frames reporting its interaction to the ligand (Fig. 1).

Due to wide movements into the hMAO-A cleft, both compounds showed a larger number of interacting residues in this isozyme (see Figures S4 and S5 in Supplementary content). The percentage of frames reporting **3g** or **3h** interacting to the FAD remarked that our ligands were located into the hMAO-B binding cleft (**3g** = 93.78%; **3h** = 92.12%) deeper than into the hMAO-A (**3g** = 82.16%; **3h** = 82.99%). Such an information suggested to investigate the stacking interaction among the phenolic ring of our compounds and the hMAO-A Tyr407 and 444 and the corresponding hMAO-B Tyr398 and 435. The compound **3g** into the hMAO-B showed stacking with both residues for more than 90% of the simulation time, while in all other cases a preference for one of the two tyrosines was observed. The stacking stability could be attributed to the **3g** *p*-methoxy phenyl group. In order to deep investigate the role of such a moiety, quantum mechanics calculations of both ligands molecular orbital were performed (Section Experimental section).

As expected, even if molecular orbital distribution of our compounds was similar, **3g** revealed HOMO/LUMO areas surrounding the *p*-methoxy phenyl ring larger than **3h** (see Figure S5 in Supplementary content) suggesting stronger interaction to the tyrosine residues. Moreover, such a substituent highlighted a different role depending on the target. In the hMAO-A *p*-

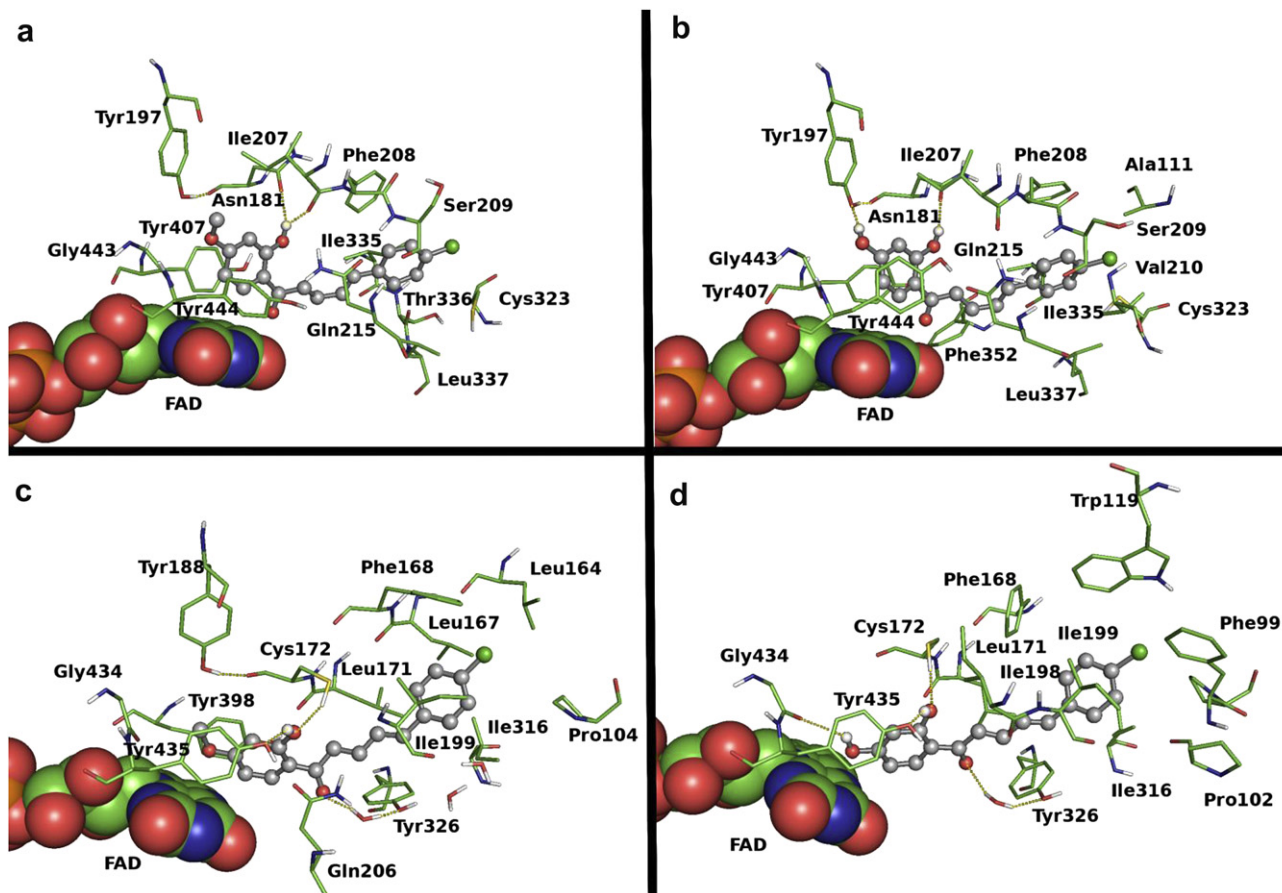


Fig. 1. Representative molecular dynamics binding modes of **3g** (left side) and **3h** (right side) into the hMAO-A (top side) and hMAO-B (bottom side) active sites. Residues interacting to the inhibitors with a frequency higher than 60% are reported in green carbons sticks or space fill, ligands are depicted in gray carbons balls and sticks. Yellow dotted lines indicate hydrogen bonds. (For interpretation of the references to color in this figure legend, the reader is referred to the web version of this article.)

methoxy phenyl ring cannot interact to Tyr197 and allowed the hydrogen bonding between **3g** *o*-phenolic group and both Asn181 side chain and Ile207 backbone. Unlike **3h**, the interaction network has forced the removal of the **3g** aromatic ring from the FAD and consequently from the Tyr407–444 stacking. Into the hMAO-B, the substitution of the Asn181 with the Cys172 was mainly responsible of our compounds isoform selectivity. In fact, the flexibility of the Cys side chain was lower than Asn and the hydrogen bond to Cys172 was unable to withdraw from the FAD both our inhibitors that, therefore, established stacking contacts to Tyr398 and 435. The hMAO-B active site, larger than hMAO-A, allowed the entrance of solvent water molecules that contributed to the complexes stabilization performing hydrogen bond bridge between the keto-group of our compounds and the Tyr326 side chain.

### 3. Conclusion

A new class of highly potent and selective hMAO-B inhibitors was identified. The most potent derivatives **3g** and **3h** showed inhibitory activity in the low nanomolar range coupled with high selectivity. Moreover, the results of reversibility tests suggest that these two compounds are reversible inhibitors of MAO-B. Based on their potent and selective MAO-B inhibitory properties, these compounds could be useful for the development of promising drug candidate for the therapy of neurodegenerative diseases.

### 4. Experimental section

#### 4.1. Chemistry

Chemicals were purchased from Sigma–Aldrich and used without further purification. Melting points were determined on a Stenford Research Systems OptiMelt (MPA-100) apparatus and are uncorrected.  $^1\text{H}$  NMR and  $^{13}\text{C}$  NMR spectra were detected with a Bruker AM-400 spectrometer, using TMS as internal standard. IR spectra were recorded on a FT-IR PerkinElmer Spectrum 1000. All compounds were routinely checked by thin-layer chromatography (TLC) and  $^1\text{H}$  NMR. TLC was performed on silica gel or aluminum oxide fluorescent coated plates (Fluka, DC-Alufolien Kieselgel or aluminum oxide F254). Compound purity was determined by elemental analysis and was confirmed to be >95% for all the tested compounds. Analytical results are within  $\pm 0.40\%$  of the theoretical values (Table 2 in Supplementary content). The synthetic intermediates 2-hydroxy-4-[(tetrahydro-2H-pyran-2-yl)oxy]acetophenone (**1f**) [12], 2-hydroxy-6-[(tetrahydro-2H-pyran-2-yl)oxy]acetophenone (**1g**) [17], (*E*)-3,4-dimethoxycinnamaldehyde (**2e**) [18], and (*E*)-3-(4-acetoxy-3-methoxy)cinnamic acid (**2f**) [19] were synthesized following the procedure previously described. (2*E*,4*E*)-1-(2-Hydroxyphenyl)-5-phenylpenta-2,4-dien-1-ones (**3a–f**, **3i**, **3k**, **3r**) [20,21], 2'-cinnamoyloxyacetophenones (**5a–e**, **5i**, **5j**) [21,22], (2*Z*,4*E*)-3-hydroxy-1-(2-hydroxyphenyl)-5-phenylpenta-2,4-dien-1-ones (**6a–e**, **6i**, **6j**, **6k**) [21,22], and (*E*)-1-(5-fluoro-2-hydroxyphenyl)-3-phenylprop-2-en-1-one (**7**) [21] were prepared as previously reported by us.

#### 4.1.1. General procedure for the synthesis of (2*E*,4*E*)-1-(2-hydroxyphenyl)-5-phenylpenta-2,4-dien-1-ones (**3j**, **3l–q**)

An aqueous solution of 60% sodium hydroxide (50 mL) was added dropwise to a stirred suspension of the appropriate 2'-hydroxyacetophenone (**1a**, **1c**, **1d**, **1g**) (10 mmol) and substituted cinnamaldehyde (**2c**, **2e**, **2f**) (11 mmol) in methanol (50 mL), cooled in ice bath. The mixture was stirred at room temperature for 48 h (**3j**, **3l**, **3m**, **3p**, **3q**) or heated at 60 °C for 5 h (**3n**, **3o**). After that period, the suspension was diluted with ice and water and acidified with 2 N hydrochloric acid. For the eventual deprotection of the

hydroxyl group (synthesis of compounds **3n–q**), the mixture was stirred at room temperature for 1 h. The resulting suspension was filtered (**3j**) or extracted with AcOEt (**3l–q**). In the latter case, the combined organic phases were washed with saturated  $\text{NaHCO}_3$  solution and brine, then dried over  $\text{Na}_2\text{SO}_4$ , filtered and evaporated to dryness. The crude product was purified by crystallization from AcOEt (**3j**) or chromatographed on a silica gel column eluting with AcOEt/petroleum ether 1:1 (**3l** and **3m**), AcOEt/petroleum ether 1:3 (**3p**), AcOEt/petroleum ether 1:4 (**3q**) or  $\text{CH}_2\text{Cl}_2$  (**3n** and **3o**).

4.1.1.1. (2*E*,4*E*)-1-(5-Fluoro-2-hydroxyphenyl)-5-(4-methoxyphenyl)penta-2,4-dien-1-one (**3j**). Yield: 78%; mp 191–193 °C from AcOEt. IR (KBr) 3450, 1620  $\text{cm}^{-1}$ .  $^1\text{H}$  NMR ( $\text{CDCl}_3$ ):  $\delta$  (ppm) 12.70 (s, 1H, OH), 7.75 (dd, 1H, H $\beta$ ,  $J_{\alpha-\beta} = 14.5$  Hz,  $J_{\beta-\gamma} = 10.3$  Hz), 7.55–7.47 (m, 3H, H $\delta$ , H $\delta'$ , H $\delta''$ ), 7.23 (dt, 1H, H $\alpha$ ,  $J_{\alpha-\beta} = 8.8$  Hz,  $J_{\alpha-\gamma} = 8.8$  Hz,  $J_{\alpha-\delta} = 2.8$  Hz), 7.12–6.86 (m, 6H, H $\gamma$ , H $\delta$ , H $\delta'$ , H $\delta''$ , H $\delta'''$ , H $\delta''''$ ), 3.87 (s, 3H, OCH $_3$ ).  $^{13}\text{C}$  NMR ( $\text{CDCl}_3$ ):  $\delta$  (ppm) 192.8 (d,  $J_{\text{C-F}} = 2.3$  Hz), 161.1, 159.7, 154.9 (d,  $J_{\text{C-F}} = 236.1$  Hz), 147.0, 143.6, 129.2, 128.7, 124.4, 123.5 (d,  $J_{\text{C-F}} = 23.7$  Hz), 121.7, 119.7 (d,  $J_{\text{C-F}} = 7.3$  Hz), 119.6 (d,  $J_{\text{C-F}} = 6.1$  Hz), 114.5, 114.4 (d,  $J_{\text{C-F}} = 21.3$  Hz), 55.4.

4.1.1.2. (2*E*,4*E*)-5-(3,4-Dimethoxyphenyl)-1-(2-hydroxyphenyl)penta-2,4-dien-1-one (**3l**). Yield: 48%; mp 193–196 °C from acetone. IR (KBr) 1632  $\text{cm}^{-1}$ .  $^1\text{H}$  NMR ( $\text{CDCl}_3$ ):  $\delta$  (ppm) 12.96 (s, 1H, 2OH), 7.84 (dd, 1H, H $\delta$ ,  $J_{5-6} = 8.1$  Hz,  $J_{4-6} = 1.6$  Hz), 7.72 (dd, 1H, H $\beta$ ,  $J_{\alpha-\beta} = 14.6$  Hz,  $J_{\beta-\gamma} = 10.6$  Hz), 7.47 (ddd, 1H, H $\alpha$ ,  $J_{4-5} = 7.2$  Hz,  $J_{3-4} = 8.5$  Hz,  $J_{4-6} = 1.6$  Hz), 7.19 (d, 1H, H $\alpha$ ,  $J_{\alpha-\beta} = 14.6$  Hz), 7.08 (dd, 1H, H $\delta'$ ,  $J_{5'-6'} = 8.3$  Hz,  $J_{2'-6'} = 1.9$  Hz), 7.05–6.86 (m, 6H, H $\gamma$ , H $\delta$ , H $\delta'$ , H $\delta''$ , H $\delta'''$ , H $\delta''''$ ), 3.95 (s, 3H, OCH $_3$ ), 3.93 (s, 3H, OCH $_3$ ).  $^{13}\text{C}$  NMR ( $\text{CDCl}_3$ ):  $\delta$  (ppm) 193.7, 163.6, 150.7, 149.4, 145.9, 143.0, 136.1, 129.4, 129.2, 124.9, 122.5, 121.7, 120.2, 118.7, 118.6, 111.3, 109.5, 56.0, 55.9.

4.1.1.3. (2*E*,4*E*)-5-(3,4-Dimethoxyphenyl)-1-(2-hydroxy-6-methoxyphenyl)penta-2,4-dien-1-one (**3m**). Yield: 48%; mp 136–139 °C from AcOEt/petroleum ether. IR (KBr) 1621  $\text{cm}^{-1}$ .  $^1\text{H}$  NMR ( $\text{CDCl}_3$ ):  $\delta$  (ppm) 13.28 (s, 1H, OH), 7.66 (dd, 1H, H $\beta$ ,  $J_{\alpha-\beta} = 14.8$  Hz,  $J_{\beta-\gamma} = 10.4$  Hz), 7.40 (d, 1H, H $\alpha$ ,  $J_{\alpha-\beta} = 14.8$  Hz), 7.34 (t, 1H, H $\alpha$ ,  $J_{3-4} = J_{4-5} = 8.3$  Hz), 7.08 (dd, 1H, H $\delta'$ ,  $J_{5'-6'} = 8.3$  Hz,  $J_{2'-6'} = 1.9$  Hz), 7.05 (d, 1H, H $\delta'$ ,  $J_{2'-6'} = 1.9$  Hz), 6.97 (d, 1H, H $\delta$ ,  $J_{\gamma-\delta} = 15.3$  Hz), 6.89 (dd, 1H, H $\gamma$ ,  $J_{\beta-\gamma} = 10.4$  Hz,  $J_{\gamma-\delta} = 15.3$  Hz), 6.86 (d, 1H, H $\delta'$ ,  $J_{5'-6'} = 8.3$  Hz), 6.60 (d, 1H, H $\delta$ ,  $J_{4-5} = 8.3$  Hz), 6.41 (d, 1H, H $\delta$ ,  $J_{3-4} = 8.3$  Hz), 3.95 (s, 3H, OCH $_3$ ), 3.94 (s, 3H, OCH $_3$ ), 3.92 (s, 3H, OCH $_3$ ).  $^{13}\text{C}$  NMR ( $\text{CDCl}_3$ ):  $\delta$  (ppm) 194.2, 164.9, 160.9, 150.4, 149.3, 144.2, 141.8, 135.6, 129.9, 129.5, 125.6, 121.5, 112.0, 111.3, 111.0, 109.5, 101.5, 55.99, 55.96, 55.85.

4.1.1.4. (2*E*,4*E*)-5-(4-Hydroxy-3-methoxyphenyl)-1-(2-hydroxyphenyl)penta-2,4-dien-1-one (**3n**). Yield: 80%; mp 124–126 °C from AcOEt/petroleum ether. IR (KBr) 3455, 1630  $\text{cm}^{-1}$ .  $^1\text{H}$  NMR ( $\text{CDCl}_3$ ):  $\delta$  (ppm) 12.96 (s, 1H, 2OH), 7.84 (dd, 1H, H $\delta$ ,  $J_{4-6} = 1.5$  Hz,  $J_{5-6} = 8.1$  Hz), 7.71 (dd, 1H, H $\beta$ ,  $J_{\alpha-\beta} = 14.6$  Hz,  $J_{\beta-\gamma} = 10.7$  Hz), 7.47 (ddd, 1H, H $\alpha$ ,  $J_{4-5} = 7.3$  Hz,  $J_{3-4} = 8.5$  Hz,  $J_{4-6} = 1.5$  Hz), 7.18 (d, 1H, H $\alpha$ ,  $J_{\alpha-\beta} = 14.6$  Hz), 7.07 (dd, 1H, H $\delta'$ ,  $J_{5'-6'} = 8.2$  Hz,  $J_{2'-6'} = 1.8$  Hz), 7.03–6.87 (m, 6H, H $\gamma$ , H $\delta$ , H $\delta'$ , H $\delta''$ , H $\delta'''$ , H $\delta''''$ ), 5.84 (s, 1H, 4'OH), 3.95 (s, 3H, OCH $_3$ ).  $^{13}\text{C}$  NMR ( $\text{CDCl}_3$ ):  $\delta$  (ppm) 193.7, 163.6, 147.5, 146.9, 146.0, 143.2, 136.1, 129.4, 128.7, 124.6, 122.2, 122.1, 120.1, 118.7, 113.6, 114.9, 109.1, 56.0.

4.1.1.5. (2*E*,4*E*)-5-(4-Hydroxy-3-methoxyphenyl)-1-(2-hydroxy-6-methoxyphenyl)penta-2,4-dien-1-one (**3o**). Yield: 58%; mp 113–115 °C from AcOEt/petroleum ether. IR (KBr) 3443, 1620  $\text{cm}^{-1}$ .  $^1\text{H}$  NMR ( $\text{CDCl}_3$ ):  $\delta$  (ppm) 13.29 (s, 1H, 2OH), 7.65 (dd, 1H, H $\beta$ ,  $J_{\alpha-\beta} = 14.8$  Hz,  $J_{\beta-\gamma} = 10.3$  Hz), 7.39 (d, 1H, H $\alpha$ ,  $J_{\alpha-\beta} = 14.8$  Hz), 7.33 (t, 1H, H $\alpha$ ,  $J_{4-5} = J_{3-4} = 8.3$  Hz), 7.06 (dd, 1H, H $\delta$ ,  $J_{5'-6'} = 8.2$  Hz,  $J_{2'-6'} = 1.9$  Hz), 7.00 (d, 1H, H $\delta'$ ,  $J_{2'-6'} = 1.9$  Hz), 6.95–6.83 (m, 3H, H $\gamma$ , H $\delta$ , H $\delta'$ ), 6.60 (dd, 1H, H $\delta$ ,  $J_{4-5} = 8.3$  Hz,  $J_{3-5} = 0.8$  Hz), 6.40 (dd, 1H,

H<sub>3</sub>, J<sub>3-4</sub> = 8.3 Hz, J<sub>3-5</sub> = 0.8 Hz), 5.83 (s, 1H, 4'OH), 3.95 (s, 3H, OCH<sub>3</sub>), 3.93 (s, 3H, OCH<sub>3</sub>). <sup>13</sup>C NMR (CDCl<sub>3</sub>): δ (ppm) 194.2, 164.9, 160.9, 147.1, 146.8, 144.3, 142.0, 135.6, 129.7, 129.0, 125.3, 121.8, 114.8, 112.0, 110.9, 109.1, 101.5, 56.0, 55.8.

4.1.1.6. (2*E*,4*E*)-1-(2,6-Dihydroxyphenyl)-5-(3,4-dimethoxyphenyl)penta-2,4-dien-1-one (**3p**). Yield: 38%; mp 185–189 °C from EtOH. IR (KBr) 3405, 1625 cm<sup>-1</sup>. <sup>1</sup>H NMR (CD<sub>3</sub>COCD<sub>3</sub>): δ (ppm) 11.58 (s, 2H, OH), 7.75–7.64 (m, 2H, H<sub>α</sub>, H<sub>β</sub>), 7.31 (d, 1H, H<sub>2'</sub>, J<sub>2'-6'</sub> = 2.0 Hz), 7.26 (t, 1H, H<sub>4</sub>, J<sub>3-4</sub> = 8.2 Hz), 7.17–7.10 (m, 3H, H<sub>γ</sub>, H<sub>δ</sub>, H<sub>6'</sub>), 6.97 (d, 1H, H<sub>5'</sub>, J<sub>5'-6'</sub> = 8.3 Hz), 6.43 (d, 2H, H<sub>3</sub>, H<sub>5</sub>, J<sub>3-4</sub> = 8.2 Hz), 3.87 (s, 3H, OCH<sub>3</sub>), 3.85 (s, 3H, OCH<sub>3</sub>). <sup>13</sup>C NMR (DMSO *D*<sub>6</sub>): δ (ppm) 194.0, 160.6, 150.2, 149.0, 144.7, 142.2, 134.8, 129.5, 129.0, 125.4, 121.8, 111.7, 111.6, 109.8, 107.1, 55.56, 55.57.

4.1.1.7. (2*E*,4*E*)-1-(2,6-Dihydroxyphenyl)-5-(4-hydroxy-3-methoxyphenyl)penta-2,4-dien-1-one (**3q**). Yield: 45%; mp 176–179 °C from AcOEt/petroleum ether. IR (KBr) 3374, 1628 cm<sup>-1</sup>. <sup>1</sup>H NMR (CD<sub>3</sub>COCD<sub>3</sub>): δ (ppm) 11.5 (s, 2H, OH), 8.05 (s, 1H, OH), 7.73–7.64 (m, 2H, H<sub>α</sub>, H<sub>β</sub>), 7.31 (d, 1H, H<sub>2'</sub>, J<sub>2'-6'</sub> = 1.9 Hz), 7.26 (t, 1H, H<sub>4</sub>, J<sub>3-4</sub> = 8.2 Hz), 7.12–7.09 (m, 3H, H<sub>γ</sub>, H<sub>δ</sub>, H<sub>6'</sub>), 6.85 (d, 1H, H<sub>5'</sub>, J<sub>5'-6'</sub> = 8.2 Hz), 6.43 (d, 2H, H<sub>3</sub>, H<sub>5</sub>, J<sub>3-4</sub> = 8.2 Hz), 3.91 (s, 3H, OCH<sub>3</sub>). <sup>13</sup>C NMR (DMSO *D*<sub>6</sub>): δ (ppm) 194.0, 160.6, 148.5, 148.0, 145.0, 142.8, 134.8, 128.9, 127.8, 124.5, 122.1, 115.6, 111.6, 110.5, 107.1, 55.7.

#### 4.1.2. Synthesis of (2*E*,4*E*)-5-(4-chlorophenyl)-1-(2-hydroxy-4-methoxyphenyl)penta-2,4-dien-1-one (**3g**)

Barium hydroxide octahydrate (15 mmol) was added to a mixture of 2-hydroxy-4-methoxyacetophenone (**1e**) (10 mmol) and 4-chlorocinnamaldehyde (**2b**) (10 mmol) in EtOH (200 mL). The mixture was stirred at 50 °C for 5 h and at room temperature overnight. After removal of ethanol in vacuum, water was added to the residue and the pH was adjusted to 2 with 2 N HCl. The mixture was extracted with AcOEt. The combined organic phases were washed with saturated NaHCO<sub>3</sub> solution and brine, then dried over Na<sub>2</sub>SO<sub>4</sub>, filtered and evaporated to dryness. The residue was purified by silica gel column chromatography eluting with AcOEt/petroleum ether 1:4. Yield: 40%; mp 182–183 °C from AcOEt. IR (KBr) 3454, 1621 cm<sup>-1</sup>. <sup>1</sup>H NMR (DMSO *D*<sub>6</sub>): δ (ppm) 13.46 (s, 1H, OH), 7.92 (d, 1H, H<sub>6</sub>, J<sub>5-6</sub> = 9.4 Hz), 7.65 (dd, 1H, H<sub>β</sub>, J<sub>α-β</sub> = 14.8 Hz, J<sub>β-γ</sub> = 8.4 Hz), 7.43 (d, 2H, H<sub>2'</sub>, H<sub>6'</sub>, J<sub>2'-3'</sub> = 8.4 Hz), 7.34 (d, 2H, H<sub>3'</sub>, H<sub>5'</sub>, J<sub>2'-3'</sub> = 8.4 Hz), 7.14 (d, 1H, H<sub>α</sub>, J<sub>α-β</sub> = 14.8 Hz), 7.03–6.94 (m, 2H, H<sub>γ</sub>, H<sub>δ</sub>), 6.48–6.45 (m, 2H, H<sub>3</sub>, H<sub>5</sub>), 3.85 (s, 3H, OCH<sub>3</sub>). <sup>13</sup>C NMR (DMSO *D*<sub>6</sub>): δ (ppm) 191.7, 166.7, 166.2, 144.0, 140.5, 135.1, 134.6, 131.1, 129.1, 128.5, 127.4, 124.3, 114.1, 107.7, 101.1, 55.6.

#### 4.1.3. Synthesis of (2*E*,4*E*)-5-(4-chlorophenyl)-1-(2,4-dihydroxyphenyl)penta-2,4-dien-1-one (**3h**)

Barium hydroxide octahydrate (15 mmol) was added to a mixture of 2-hydroxy-4-[(tetrahydro-2*H*-pyran-2-yl)oxy]acetophenone (**1g**) [12] (10 mmol) and 4-chlorocinnamaldehyde (**2b**) (10 mmol) in EtOH (200 mL). The mixture was stirred at 50 °C for 5 h and at room temperature overnight. After removal of ethanol in vacuum, water was added to the residue, the pH was adjusted to 2 with 2 N HCl, and the mixture was stirred at room temperature for 1 h. After this period, the solid was removed by filtration, washed with water and purified by silica gel column chromatography eluting with AcOEt/petroleum ether 1:4. Yield: 61%; mp 217–220 °C from AcOEt/petroleum ether. IR (KBr) 3440, 3241, 1636 cm<sup>-1</sup>. <sup>1</sup>H NMR (DMSO *D*<sub>6</sub>): δ (ppm) 13.36 (s, 1H, OH), 10.80 (bs, 1H, OH), 7.92 (d, 1H, H<sub>6</sub>, J<sub>5-6</sub> = 8.9 Hz), 7.62 (d, 2H, H<sub>2'</sub>, H<sub>6'</sub>, J<sub>2'-3'</sub> = 8.4 Hz), 7.58 (dd, 1H, H<sub>β</sub>, J<sub>α-β</sub> = 14.8 Hz, J<sub>β-γ</sub> = 9.6 Hz), 7.50–7.46 (m, 3H, H<sub>α</sub>, H<sub>3'</sub>, H<sub>5'</sub>), 7.27 (dd, 1H, H<sub>γ</sub>, J<sub>γ-δ</sub> = 15.5 Hz, J<sub>β-γ</sub> = 9.6 Hz), 7.22 (d, 1H, H<sub>δ</sub>, J<sub>γ-δ</sub> = 15.5 Hz), 6.42 (dd, 1H, H<sub>5</sub>, J<sub>5-6</sub> = 8.9 Hz, J<sub>3-5</sub> = 2.3 Hz), 6.30 (d, 1H, H<sub>3</sub>, J<sub>3-5</sub> = 2.3 Hz). <sup>13</sup>C NMR (DMSO *D*<sub>6</sub>): δ (ppm) 191.1, 165.6,

165.1, 143.5, 140.1, 134.9, 133.6, 132.3, 128.9, 128.8, 127.9, 125.1, 112.9, 108.3, 102.6.

#### 4.1.4. General procedure for the synthesis of 2-acetylphenyl (*E*)-cinnamates (**5f–h**)

Phosphorus oxychloride (30 mmol) were added to a solution of the appropriate 2-hydroxyacetophenone (**1a**, **1d**) (10 mmol) and substituted cinnamic acid (**4f**, **4g**) (12 mmol) in dry pyridine (20 mL) cooled in ice bath. The solution was stirred at room temperature for 4 h, then it was poured into ice and water and acidified with 2 N HCl. The precipitate was removed by filtration, washed with water and purified by silica gel column chromatography eluting with AcOEt/light petroleum (1:3).

4.1.4.1. 2-Acetylphenyl (*E*)-3,4-dimethoxycinnamate (**5f**). Yield: 73%; mp 102–104 °C from EtOH. The compound exhibited spectroscopic data identical to those previously reported [23].

4.1.4.2. 2-Acetyl-3-methoxyphenyl (*E*)-3,4-dimethoxycinnamate (**5g**). Yield: 90%; mp 96–98 °C from EtOH. The compound exhibited spectroscopic data identical to those previously reported [23].

4.1.4.3. 2-Acetyl-3-methoxyphenyl (*E*)-4-acetoxy-3-methoxycinnamate (**5h**). Yield: 48%; mp 143–146 °C from AcOEt/petroleum ether. IR (KBr) 1767, 1715, 1633 cm<sup>-1</sup>. <sup>1</sup>H NMR (CDCl<sub>3</sub>): δ (ppm) 7.78 (d, 1H, H<sub>β</sub>, J<sub>α-β</sub> = 15.9 Hz), 7.38 (t, 1H, H<sub>5</sub>, J<sub>4-5</sub> = J<sub>5-6</sub> = 8.3 Hz), 7.18–7.14 (m, 2H, H<sub>6'</sub>, H<sub>2'</sub>), 7.07 (d, 1H, H<sub>5'</sub>, J<sub>5'-6'</sub> = 8.4 Hz), 6.85 (d, 1H, H<sub>4</sub>, J<sub>4-5</sub> = 8.3 Hz), 6.81 (d, 1H, H<sub>6</sub>, J<sub>3-4</sub> = 8.3 Hz), 6.52 (d, 1H, H<sub>α</sub>, J<sub>α-β</sub> = 15.9 Hz), 3.89 (s, 3H, OCH<sub>3</sub>), 3.90 (s, 3H, OCH<sub>3</sub>), 2.51 (s, 3H, COCH<sub>3</sub>), 2.32 (s, 3H, OCOCH<sub>3</sub>).

#### 4.1.5. General procedure for the synthesis of (2*Z*,4*E*)-3-hydroxy-1-(2-hydroxyphenyl)-5-phenylpenta-2,4-dien-1-ones (**6f**, **6g**)

Anhydrous K<sub>2</sub>CO<sub>3</sub> (50 mmol) was added to a solution of the appropriate 2-acetylphenyl (*E*)-cinnamate (**5f**, **5g**) (10 mmol) in dry acetone (100 mL), and the mixture was refluxed for 24 h with stirring. After cooling, the mixture was poured into ice and the pH was adjusted to 4 with 2 N HCl. The solid was removed by filtration, dissolved in chloroform and washed with brine. The organic phase was dried over Na<sub>2</sub>SO<sub>4</sub>, filtered and evaporated to dryness. The residue was purified by crystallization.

4.1.5.1. (2*Z*,4*E*)-5-(3,4-Dimethoxyphenyl)-3-hydroxy-1-(2-hydroxyphenyl)penta-2,4-dien-1-one (**6f**). Yield: 40%; mp 126–128 °C from EtOH. The compound exhibited spectroscopic data identical to those previously reported [23].

4.1.5.2. (2*Z*,4*E*)-5-(3,4-Dimethoxyphenyl)-3-hydroxy-1-(2-hydroxy-6-methoxyphenyl)penta-2,4-dien-1-one (**6g**). Yield: 40%; mp 131–132 °C from AcOEt. The compound exhibited spectroscopic data identical to those previously reported [23].

#### 4.1.6. (2*Z*,4*E*)-3-Hydroxy-5-(4-hydroxy-3-methoxyphenyl)-1-(2-hydroxy-6-methoxyphenyl)penta-2,4-dien-1-one (**6h**)

Anhydrous K<sub>2</sub>CO<sub>3</sub> (50 mmol) was added to a solution of 2-acetyl-3-methoxyphenyl (*E*)-3-(4-acetoxy-3-methoxyphenyl)cinnamate (**5h**) (10 mmol) in dry acetone (100 mL), and the mixture was refluxed for 24 h with stirring. After cooling, the mixture was poured into ice (50 g) and water (50 mL), and stirred at room temperature for 1 h. After that period, the pH was adjusted to 4 with 2 N HCl, the solid was removed by filtration and purified by silica gel column chromatography eluting with CH<sub>2</sub>Cl<sub>2</sub>. Yield: 25%; mp 162–164 °C from AcOEt/petroleum ether. IR (KBr) 3406, 1626 cm<sup>-1</sup>. <sup>1</sup>H NMR (CDCl<sub>3</sub>): δ (ppm) (CDCl<sub>3</sub>): 14.85 (s, 1H, OH), 12.77 (s, 1H, OH), 7.58 (d, 1H, H<sub>δ</sub>, J<sub>γ-δ</sub> = 15.8 Hz), 7.32 (t, 1H, H<sub>4</sub>, J<sub>3-</sub>

$4 = J_{4-5} = 8.3$  Hz), 7.15 (dd, 1H, H6',  $J_{5'-6'} = 8.2$  Hz,  $J_{2'-6'} = 1.9$  Hz), 7.06 (d, 1H, H2',  $J_{2'-6'} = 1.9$  Hz), 6.95 (d, 1H, H5',  $J_{5'-6'} = 8.2$  Hz), 6.77 (s, 1H, H $\alpha$ ), 6.60 (d, 1H, H3,  $J_{3-4} = 8.3$  Hz), 6.45 (d, 1H, H $\gamma$ ,  $J_{\gamma-\delta} = 15.8$  Hz), 6.43 (d, 1H, H5,  $J_{4-5} = 8.3$  Hz), 5.99 (s, 1H, OH), 3.97 (s, 3H, OCH<sub>3</sub>), 3.96 (s, 3H, OCH<sub>3</sub>). <sup>13</sup>C NMR (CDCl<sub>3</sub>):  $\delta$  (ppm) 194.7, 175.2, 164.0, 160.3, 147.8, 146.8, 139.6, 134.9, 127.9, 122.7, 120.4, 114.9, 111.1, 110.7, 109.7, 103.2, 101.7, 56.0, 55.9.

#### 4.1.7. (2Z,4E)-5-(3,4-Dihydroxyphenyl)-3-hydroxy-1-(2-hydroxyphenyl)penta-2,4-dien-1-one (**6m**)

A solution 1 M of boron tribromide in dichloromethane (100 mL) was added dropwise to a stirred solution of **6f** (10 mmol) in dry dichloromethane (200 mL) cooled in ice bath. The reaction mixture was stirred in ice bath for 1 h and then at room temperature for 20 h. After this period, the mixture was poured into ice and water and vigorously stirred. The obtained precipitate was filtered, washed with water, and purified by silica gel column chromatography eluting with AcOEt/petroleum ether 1:1. Yield: 40%; mp 200–201 °C from AcOEt. IR (KBr) 3385, 1635 cm<sup>-1</sup>. <sup>1</sup>H NMR (acetone *d*<sub>6</sub>):  $\delta$  (ppm) 14.73 (s, 1H, OH), 12.21 (s, 1H, OH), 8.45 (bs, 2H, 2OH), 7.92 (dd, 1H, H6,  $J_{5-6} = 8.3$  Hz,  $J_{4-6} = 1.5$  Hz), 7.60 (d, 1H, H $\delta$ ,  $J_{\gamma-\delta} = 15.8$  Hz), 7.51 (ddd, 1H, H4,  $J_{3-4} = 8.4$  Hz,  $J_{4-5} = 7.2$  Hz,  $J_{4-6} = 1.5$  Hz), 7.21 (d, 1H, H2',  $J_{2'-6'} = 2.0$  Hz), 7.09 (dd, 1H, H6',  $J_{5'-6'} = 8.2$  Hz,  $J_{2'-6'} = 2.0$  Hz), 6.97–6.94 (m, 2H, H3, H5), 6.90 (d, 1H, H5',  $J_{5'-6'} = 8.2$  Hz), 6.69 (d, 1H, H $\gamma$ ,  $J_{\gamma-\delta} = 15.8$  Hz), 6.68 (s, 1H, H $\alpha$ ). <sup>13</sup>C NMR (DMSO *D*<sub>6</sub>):  $\delta$  (ppm) 191.4, 177.7, 159.9, 148.5, 145.7, 140.5, 134.9, 129.2, 126.3, 121.6, 120.1, 119.2, 117.7, 115.8, 114.7, 114.4, 98.5.

## 4.2. Biochemistry

### 4.2.1. Determination of hMAO isoform activity

The effects of the tested compounds on hMAO isoform enzymatic activity were evaluated by measuring their effects on the production of hydrogen peroxide from *p*-tyramine using the Amplex Red MAO assay kit (Molecular Probes, Inc., Eugene, Oregon, USA) and microsomal MAO isoforms prepared from insect cells (BT1-TN-5B1-4) infected with recombinant baculovirus containing cDNA inserts for hMAO-A or hMAO-B (Sigma–Aldrich Química S.A., Alcobendas, Spain). Briefly, various concentrations of the test drugs or reference inhibitors and adequate amounts of recombinant hMAO-A or hMAO-B (required to obtain the same reaction velocity) were incubated for 15 min at 37 °C in a sodium phosphate buffer (0.05 M, pH 7.4). The reaction was started by adding (final concentrations) 200  $\mu$ M Amplex Red reagent, 1 U/mL horseradish peroxidase and 1 mM *p*-tyramine which is totally sufficient to saturate both MAO isoforms in these experimental conditions. The hMAO activity was evaluated by measuring the fluorescence generated by resorufin using the general procedure described previously by us [14]. The possible capacity of the above test drugs to modify the fluorescence due to non-enzymatic inhibition (e.g., for directly reacting with Amplex Red reagent) was determined by adding these drugs to solutions containing only the Amplex Red reagent in a sodium phosphate buffer. For fluorescent compounds, incubations with 60  $\mu$ M kynuramine (Sigma–Aldrich Química S.A., Alcobendas, Spain) were performed at 37 °C and pH 7.4 in a sodium phosphate buffer (Na<sub>2</sub>HPO<sub>4</sub>/KH<sub>2</sub>PO<sub>4</sub> isotoned with KCl). The rate of oxidation of the non selective substrate into 4-hydroxyquinolone was monitored at 314 nm using a Pharmacia Biotech Ultrospec 4000 UV/Visible Spectrophotometer [24]. IC<sub>50</sub> values were estimated by non-linear regression analysis using GraphPad Prism software (San Diego, USA), with  $X = \log$  molar concentration of tested compound and  $Y = \text{percentage of inhibition of control resorufin production}$ . This regression was performed using data obtained with 4–6 different concentrations of each tested compound. IC<sub>50</sub> values are the mean  $\pm$  S.E.M. from five experiments.

### 4.2.2. Reversibility and irreversibility experiments

To evaluate whether some of the tested compounds (**3b**, **3g**, **3h**, **6d** and **6k**) are reversible or irreversible hMAO-B inhibitors, an effective centrifugation–ultrafiltration method (so-called repeated washing) was used [12].

### 4.3. Molecular modeling

Theoretical 3D models of the most active and hMAO-B selective compounds, **3g** and **3h** were built by means of Maestro [25] GUI version 9.1. The inhibitor structures were optimized by means of energy minimization carried out with the OPLS-2005 force field [26] and the GB/SA [27] water implicit solvation model. All these preliminary calculation were computed by the version 9.8 of the MacroModel [28] software. Docking simulation was performed using the ligand flexible algorithm of Glide [29] at XP precision level. The target models of hMAO-A and hMAO-B were two high resolution crystal structures corresponding to the Protein Data Bank codes 2Z5X [2] and 2V5Z [3] respectively. Co-crystallized ligands, harmine for 2Z5X and safinamide for 2V5Z, and water molecules were removed from both target models and their binding clefts were defined by means of a regular box of about 1000 Å<sup>3</sup>, centered onto the N5 FAD cofactor. Molecular dynamics (MD) simulations were carried out, up to 12 ns at 300 K, applying the version 2.4 of the DESMOND [30] package and the OPLS-AA force field onto the most stable complex of both inhibitors in hMAO-A and -B. The explicit solvation model TIP3 was adopted for taking into account water solvent effects. The four MD trajectories, each consisting of 240 structures sampled at regular interval equal to 5 ps, were graphical inspected and analyzed using VMD version 1.8.7 [31]. The molecular orbital (MO) analysis of compounds **3g** and **3h** was carried out at DFT level of theory using the hybrid functional B3LYP and the 6-31G\*\* basis set. For mimicking the enzyme environment, the implicit solvation model PBF chloroform was adopted. The structure of both inhibitors, selected for the MO study, were obtained from the last molecular dynamics sampled frame and energy minimized during the DFT calculation. Quantum mechanics calculations were performed by means of the Jaguar [32]. Molecular modeling figures were depicted by PyMol version 1.3 [33].

## Acknowledgments

This work was supported by the Italian MIUR (Ministero dell'Istruzione, dell'Università e della Ricerca). We thank dr Ivano Pindinello for technical assistance.

## Appendix A. Supplementary data

Supplementary data related to this article can be found at <http://dx.doi.org/10.1016/j.ejmech.2012.11.006>.

## References

- J.C. Shih, K. Chen, M.J. Ridd, Monoamine oxidase: from genes to behaviour, *Annu. Rev. Neurosci.* 22 (1999) 197–217.
- S.Y. Son, J. Ma, Y. Kondou, M. Yoshimura, E. Yamashita, T. Tsukihara, Structure of human monoamine oxidase A at 2.2-Å resolution: the control of opening the entry for substrates/inhibitors, *Proc. Natl. Acad. Sci. U. S. A.* 105 (2008) 5739–5744.
- C. Binda, J. Wang, L. Pisani, C. Caccia, A. Carotti, P. Salvati, D.E. Edmondson, A. Mattevi, Structures of human monoamine oxidase B complexes with selective noncovalent inhibitors: safinamide and coumarin analogs, *J. Med. Chem.* 50 (2007) 5848–5852.
- M.B. Youdim, D.E. Edmondson, K.F. Tipton, The therapeutic potential of monoamine oxidase inhibitors, *Nat. Rev. Neurosci.* 7 (2006) 295–309.
- M. Yamada, H. Yasuhara, Clinical pharmacology of MAO inhibitors: safety and future, *Neurotoxicology* 25 (2004) 215–221.

- [6] B. Drukarch, F.L. Van Muiswinkel, Drug treatment of Parkinson's disease. Time for phase II, *Biochem. Pharmacol.* 59 (2000) 1023–1031.
- [7] A.H. Schapira, Treatment options in the modern management of Parkinson disease, *Arch. Neurol.* 64 (2007) 1083–1088.
- [8] P. Riederer, W. Danielczyk, E. Grunblatt, Monoamine oxidase-B inhibition in Alzheimer's disease, *Neurotoxicology* 25 (2004) 271–277.
- [9] T. Thomas, Monoamine oxidase-B inhibitors in the treatment of Alzheimer's disease, *Neurobiol. Aging* 21 (2000) 343–348.
- [10] F. Chimenti, R. Fioravanti, A. Bolasco, P. Chimenti, D. Secci, F. Rossi, M. Yanez, F. Orallo, F. Ortuso, S. Alcaro, A new series of flavones, thioflavones, and flavanones as selective monoamine oxidase-B inhibitors, *Bioorg. Med. Chem.* 18 (2010) 1273–1279.
- [11] N. Desideri, A. Bolasco, R. Fioravanti, L. Proietti Monaco, F. Orallo, M. Yáñez, F. Ortuso, S. Alcaro, Homoisoflavonoids: natural scaffold with potent and selective monoamine oxidase-B inhibition properties, *J. Med. Chem.* 54 (2011) 2155–2164.
- [12] F. Chimenti, R. Fioravanti, A. Bolasco, P. Chimenti, D. Secci, F. Rossi, M. Yáñez, F. Orallo, F. Ortuso, S. Alcaro, Chalcones: a valid scaffold for monoamine oxidases inhibitors, *J. Med. Chem.* 52 (2009) 2818–2824.
- [13] C. Binda, M. Li, F. Hubalek, N. Restelli, D.E. Edmondson, A. Mattevi, Insights into the mode of inhibition of human mitochondrial monoamine oxidase B from high-resolution crystal structures, *Proc. Natl. Acad. Sci. U. S. A.* 100 (2003) 9750–9755.
- [14] M. Yáñez, N. Fraiz, E. Cano, F. Orallo, Inhibitory effects of cis- and trans-resveratrol on noradrenaline and 5-hydroxytryptamine uptake and on monoamine oxidase activity, *Biochem. Biophys. Res. Commun.* 344 (2006) 688–695.
- [15] F. Chimenti, E. Maccioni, D. Secci, A. Bolasco, P. Chimenti, A. Granese, S. Carradori, S. Alcaro, F. Ortuso, M. Yáñez, F. Orallo, R. Cirilli, R. Ferretti, F. La Torre, Synthesis, stereochemical identification, and selective inhibitory activity against human monoamine oxidase-B of 2-methylcyclohexylidene-(4-arylthiazol-2-yl)hydrazones, *J. Med. Chem.* 51 (2008) 4874–4880.
- [16] D.E. Edmondson, C. Binda, J. Wang, A.K. Upadhyay, A. Mattevi, Molecular and mechanistic properties of the membrane-bound mitochondrial monoamine oxidases, *Biochemistry* 20 (2009) 4220–4230.
- [17] M. Deodhar, D.StC. Black, N. Kumar, Acid catalyzed stereoselective rearrangement and dimerization of flavenes: synthesis of dependensin, *Tetrahedron* 63 (2007) 5227–5235.
- [18] A.I. Vedernikov, S.P. Gromov, Convenient method for the preparation of crown ether cinnamaldehydes, *Synthesis* (2001) 889–892.
- [19] A.M. Condo Jr., D.C. Baker, R.A. Moreau, K.B. Hicks, Improved method for the synthesis of trans-feruloyl-b-sitostanol, *J. Agric. Food Chem.* 49 (2001) 4961–4964.
- [20] N. Desideri, P. Mastromarino, C. Conti, Synthesis and evaluation of anti-rhinovirus activity of 3-hydroxy and 3-methoxy 2-styrylchromones, *Antivir. Chem. Chemother.* 14 (2003) 195–203.
- [21] C. Conti, P. Mastromarino, P. Goldoni, G. Portalone, N. Desideri, Synthesis and anti-rhinovirus properties of fluoro-substituted flavonoids, *Antivir. Chem. Chemother.* 16 (2005) 267–276.
- [22] N. Desideri, C. Conti, P. Mastromarino, F. Mastropaolo, Synthesis and anti-rhinovirus activity of 2-styrylchromones, *Antivir. Chem. Chemother.* 11 (2000) 321–327.
- [23] C.M.M. Santos, A.M.S. Silva, J.A.S. Cavaliero, Efficient syntheses of new polyhydroxylated 2,3-diaryl-9H-xanthen-9-ones, *Eur. J. Org. Chem.* (2009) 2642–2660.
- [24] U. Thull, S. Kneubühler, B. Testa, M.F. Borges, M.M. Pinto, Substituted xanthenes as selective and reversible monoamine oxidase A (MAO-A) inhibitors, *Pharm. Res.* 10 (1993) 1187–1190.
- [25] Maestro, Version 9.1, Schrodinger, LLC, New York, NY, 2010.
- [26] G. Kaminski, R.A. Friesner, J. Tirado-Rives, W.L. Jorgensen, Evaluation and reparametrization of the OPLS-AA force field for proteins via comparison with accurate quantum chemical calculations on peptides, *J. Phys. Chem. B* 105 (2001) 6474–6487.
- [27] W. Hasel, T.F. Hendrickson, W.C. Still, A rapid approximation to the solvent accessible surface areas of atoms, *Tetrahedron Comput. Methodol.* 1 (1988) 103–116.
- [28] (a) MacroModel, Version 9.8, Schrodinger, LLC, New York, NY, 2010; (b) F. Mohamadi, N.G.J. Richards, W.C. Guida, R. Liskamp, M. Lipton, C. Caufield, G. Chang, T. Hendrickson, W.C. Still, MacroModel—an integrated software system for modeling organic and bioorganic molecules using molecular mechanics, *J. Comput. Chem.* 11 (1990) 440–467.
- [29] (a) Glide, Version 5.6, Schrodinger, LLC, New York, NY, 2010; (b) R.A. Friesner, J.L. Banks, R.B. Murphy, T.A. Halgren, J.J. Klicic, D.T. Mainz, M.P. Repasky, E.H. Knoll, D.E. Shaw, M. Shelley, J.K. Perry, P. Francis, P.S. Shenkin, Glide: a new approach for rapid, accurate docking and scoring. 1. Method and assessment of docking accuracy, *J. Med. Chem.* 47 (2004) 1739–1749; (c) T.A. Halgren, R.B. Murphy, R.A. Friesner, H.S. Beard, L.L. Frye, W.T. Pollard, J.L. Banks, Glide: a new approach for rapid, accurate docking and scoring. 2. Enrichment factors in database screening, *J. Med. Chem.* 47 (2004) 1750–1759; (d) R.A. Friesner, R.B. Murphy, M.P. Repasky, L.L. Frye, J.R. Greenwood, T.A. Halgren, P.C. Sanschagrin, D.T. Mainz, Extra precision Glide: docking and scoring incorporating a model of hydrophobic enclosure for protein–ligand complexes, *J. Med. Chem.* 49 (2006) 6177–6196.
- [30] K.J. Bowers, E. Chow, H. Xu, R.O. Dror, M.P. Eastwood, B.A. Gregersen, J.L. Klepeis, I. Kolossváry, M.A. Moraes, F.D. Sacerdoti, J.K. Salmon, Y. Shan, D.E. Shaw, Scalable algorithms for molecular dynamics simulations on commodity clusters, in: *Proceedings of the ACM/IEEE Conference on Supercomputing (SC06)*, Tampa, Florida, November 2006, pp. 11–17.
- [31] W. Humphrey, A. Dalke, K. Schulten, VMD—visual molecular dynamics, *J. Mol. Graph.* 14 (1996) 33–38.
- [32] Jaguar, Version 5.6, Schrodinger, LLC, New York, NY, 2010.
- [33] The PyMOL Molecular Graphics System, Version 1.3, Schrödinger, LLC.